Selection of reference-anisotropy parameters for wavefield extrapolation by Lloyd's algorithm

Yaxun Tang and Robert G. Clapp, Stanford University*

SUMMARY

We propose a method for selecting reference-anisotropy parameters in laterally varying anisotropic media for mixed Fourier-space domain wavefield extrapolation. We treat the selection problem as a quantization procedure, and use a modified version of the 3D Lloyd's algoritm for reference-parameter selections. We demonstrate that our method yields a more accurate discription of the anisotropy model with fewer reference parameters than the uniform sampling approach. Synthetic and real data examples illustrate the performance of our method.

INTRODUCTION

It is well known that wavefield-continuation-based migration methods are better able to image areas affected by multi-pathing and are more effective in handling complex wave behavior than ray-tracing-based Kirchhoff methods. However, wave-equation depth migration such as PSPI (Gazdag and Sguazzero, 1984), extended SSF (Stoffa et al., 1990; Kessinger, 1992), split-step DSR (Popovici, 1996), or FFD plus interpolation (Biondi, 2002) require multiple reference velocities for wavefield extrapolation through laterally inhomogeneous velocity models. With multiple reference velocities higher angles can be accurately handled and the quality of the image can be improved, but the cost of the migration is increased in proportion to the number of reference velocities used.

When it comes to anisotropic media, the vertical wavenumber k_z becomes a function of three anisotropy parameters (v, δ and ε (or η)). To extrapolate wavefields in Fourier domain, we must use not only multiple reference velocities, but also multiple reference δs and εs (or ηs). The computational cost subsequently increases significantly. The conventional method (Rousseau, 1997; Baumstein and Anderson, 2003) for selecting those three parameters is first to uniformly sample the vertical velocity v at each depth level, then for each vertical velocity, to uniformly sample a range of δs and ηs (or εs) from their minima to their maxima. The main drawback of this method is that it may undersample the parameters at places where the lateral variations are significant, or it may oversample the parameters at places where the model is smooth. To get a better result it may require a large number of reference parameters, which is impractical for migrating large data sets.

Clapp (2004) borrowed the idea of quantization from the field of electrical engineering, and used the 1D Lloyd's algorithm to select reference velocities for isotropic migration. He demonstrated that reference velocities selected by Lloyd's algorithm can produce higher-quality images while using fewer reference velocities. In fact, the 1D Lloyd's algorithm (Lloyd, 1982) is a special case of the clustering method, which tries to find the global optimum solutions according to some statistical criteria. It can be easily extended to multi-dimensional case to accurately describe the vector field (Clapp, 2006). In this paper we use the 3D version of Lloyd's algorithm to select the reference-anisotropy parameters for wavefield extrapolation in laterally varying VTI media. We show that, by incorporating the 3D Lloyd's algorithm, we significantly reduce the computational cost and obtain high-quality images.

GENERALIZED LLOYD'S ALGORITHM

The concept of quantization originates in the field of electrical engineering. The basic idea behind quantization is to describe a continuous function, or one with a large number of samples, by a few representative values. Let x denote the input signal and $\hat{x} = Q(x)$ denote quantized values, where $Q(\cdot)$ is the quantizer mapping function. There will certainly be a distortion if we use $\hat{x}$ to represent x. In the least-square sense, the distortion can be measeured by

$$D = \int_{-\infty}^{\infty} (x - Q(x))^2 f(x) dx, \tag{1}$$

where $f(x)$ is the probability density function of the input signal (assuming the input signal is a random sequence). Consider the situation with L quantizers $\hat{x} = (\hat{x}_1, \hat{x}_2, \cdots, \hat{x}_L)$. Let the corresponding quantization intervals be

$$T_i = (a_{i-1}, a_i), i = 1, 2, \ldots, L, \tag{2}$$

where $a_0 = -\infty$ and $a_L = \infty$. Then

$$D = \int_{-\infty}^{\infty} (x - Q(x))^2 f(x) dx = \sum_{i=1}^{L} \int_{T_i} (x - \hat{x}_i)^2 f(x) dx. \tag{3}$$

In the discrete case, equation (3) can be written as follows:

$$D = \sum_{i=1}^{L} \sum_{x=a_{i-1}}^{a_i} P(x)(x - \hat{x}_i)^2, \tag{4}$$

where $P(x)$ is the discrete version of the probability density function, or normalized histogram ($\sum_x P(x) = 1$). To minimize the distortion function D, we take derivatives of equation (4) with respect to $\hat{x}_i$, a_i and set them equal to zero, leading to the following conditions for the optimum quantizers $\hat{x}_i$ and quantization interval boundaries $\hat{a}_i$:

$$\hat{a}_i = \frac{\hat{x}_i + \hat{x}_{i+1}}{2}, \tag{5}$$

$$\hat{x}_i = \frac{\sum_{x=\hat{a}_{i-1}}^{\hat{a}_i} P(x) x}{\sum_{x=\hat{a}_{i-1}}^{\hat{a}_i} P(x)}. \tag{6}$$

A way to solve this coupled set of nonlinear equations is to first generate an initial set $\{x_1, x_2, \ldots, x_L\}$, then apply equations (5) and (6) alternately until convergence is obtained. This iteration is well known as the Lloyd-Max quantization algorithm (LMQ).

It is fairly straightforward to extend the LMQ to 3D. The main extension of the approach is to break the input data points into 3D clusters instead of 1D cells. A 1D normalized histogram should be replaced with a 3D normalized histogram and a 3D distortion function should be calculated as follows:

$$D = \sum_{m=1}^{L} \left(\sum_{x=a_{i-1}}^{a_i} \sum_{y=b_{j-1}}^{b_j} \sum_{z=c_{k-1}}^{c_k} P(x,y,z)(\mathbf{r} - \hat{\mathbf{r}}) \cdot (\mathbf{r} - \hat{\mathbf{r}}) \right), \tag{7}$$

where $\hat{\mathbf{r}} = (\hat{x}_m, \hat{y}_m, \hat{z}_m)$ is the center of cluster m, $P(x,y,z)$ is the 3D histogram at point $\mathbf{r} = (x,y,z)$ within cluster m, and (a_{i-1}, a_i), (b_{j-1}, b_j), (c_{k-1}, c_k) define the boundaries of cluster m. Conditions (5) and (6) accordingly become:

1. Classification of the points. The Euclidian distance between a point and every cluster center (i.e. quantizer) is calculated. The point is assigned to the closest cluster center.

2. Updating of the quantizers. Each quantizer is the center of mass of all points which are assigned to the cluster.

It should be pointed out that LMQ is highly dependent on the initial guess and can easily get stuck in local minima. One simple but effective way to avoid these problems is to start with a uniform quantizer, and when a cluster becomes empty, replace it by splitting regions with high variance (Clapp, 2004). The detailed implementation of the modified 3D Lloyd's algorithm is discussed by Clapp (2006).

SELECTING REFERENCE-ANISOTROPY PARAMETERS

Anisotropy has been shown to exist in many sedimentary rocks (Thomsen, 1986). Most sedimentary rocks can be approximated by a transversely isotropic medium with a plane of symmetry. For vertically transversely isotropic (VTI) media, if we assume that the S-wave velocity is much smaller than the P-wave velocity, the dispersion relation can be computed as follows (Tsvankin, 2001):

$$k_z(v,\delta,\eta) = \frac{\omega}{v}\sqrt{\frac{\frac{\omega^2}{v^2}-k_x^2(1+2\varepsilon)}{\frac{\omega^2}{v^2}-2k_x^2\eta(1+2\delta)}}, \quad (8)$$

$$\eta = \frac{\varepsilon-\delta}{1+2\delta}, \quad (9)$$

where v, δ, ε (and η) are the anisotropy parameters (Thomsen, 1986; Tsvankin, 2001). In the VTI media, the vertical wavenumber k_z is a function not only of vertical velocity v, but also of δ and η (or ε), which means that for one depth-level extrapolation, three parameters should be used instead of one.

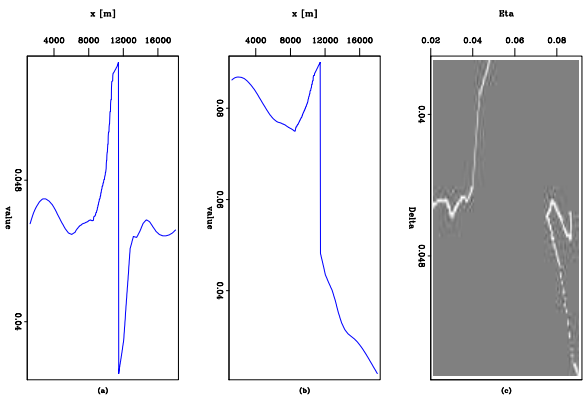

Figure 1: The values of δ, η for a single depth slice and their 2D histogram. The values of (a) δ at depth=990m and (b) η at depth=990m; (c) the 2D histogram computed from (a) and (b), the curves indicate the 2D distribution of δ and η.

The 3D Lloyd's algorithm can be easily translated into the problem of selecting reference-anisotropy parameters, because these three anisotropy parameters are correlated to some extent and have similar distributions. These properties make the selection by Lloyd's algorithm quite effective. In our selection problem, we form the parameter vector $\mathbf{r} = (v,\delta,\eta)$ or $\mathbf{r} = (v,\delta,\varepsilon)$. Now the center of the 3D mass within a cluster is the reference-parameter vector $\hat{\mathbf{r}}$, and

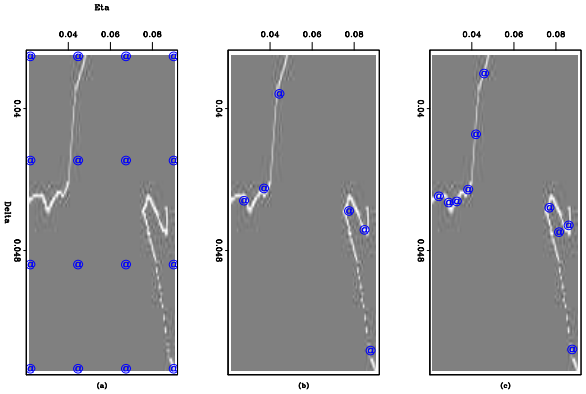

Figure 2: Comparison between the uniform sampling method and the modified 2D Lloyd's algorithm. (a) The result of uniform sampling, overlaid with the 2D histogram from Figure 1(c); (b) the result of the modified 2D Lloyd's algorithm after 2 iterations and (c) after 20 interations. Note how accurately (b) and (c) characterize the distribution of δ and η.

the boundaries of the 3D cluster define the regions with the same v, δ and η (or ε).

We test our methodology on a real data set provided by ExxonMobil. As the 3D Lloyd's algorithm is hard to visualize, we show only a 2D procedure for selecting δ and η. Figures 1(a) and 1(b) are the input δ and η for a single depth level respectively. Figure 1(c) is their 2D histogram, where the horizontal axis is η, the vertical axis is δ, and the amplitude is the value of the 2D histogram. Figure 2(a) shows the result by uniform sampling, where 16 uniformly-selected points (4 δs and 4 ηs) are overlaid with the 2D histogram (Figure 1(c)). It is quite clear that the points selected by the uniform sampling do not match well the distribution of δ and η. Figure 2(b) shows the result by using the modified Lloyd's alogrithm after 2 iterations, while Figure 2(c) is the result after 20 iterations. Note how well the result characterizes the 2D distribution of δ and η, and also note that after 20 iterations the number of (δ,η) is reduced from 16 to 10. Thus for this depth level and a given vertical velocity, we only need 10 depth extrapolations instead of 16, reducing the computational cost by almost 40 percent.

MIGRATION RESULTS

To test the migration results we apply our methodology on a synthetic 2D zero-offset data set provided by Amerada Hess and a 2D prestack real data set provided by ExxonMobil. Figure 3 shows the synthetic anistropy model for VTI media. Figure 3(a) is the vertical velocity model, Figure 3(b) is the δ model and Figure 3(c) is the ε model. For the uniform sampling method, we uniformly select three vs, δs and εs separately. For the 3D Lloyd's method, we also start with three vs, three δs and three εs as the initial input and we set the maximum number of anisotropy parameters equal to 27 for each depth level, which guarantees that the number of parameters selected by the 3D Lloyd's algorithm will be no larger than that obtained by the uniform sampling. Then we downward continuate the zero-offset data set for each reference-parameter vector with the anisotropic SSF extrapolator and a nearest neighbour interpolation is implemented to generate a single wavefield at each depth level. During the imaging process, most of the computation time is spent on the downward continuation step. For this paticular case with the total number of depth levels $nz = 1,501$, we must perform $1501 \times 27 = 40,527$ downward continuations for an uniform sampling of reference parameters. After selecting by the 3D Lloyd's

algorithm, however, the total number of downward continuations reduces to 4,401, reducing the computation time by about 90%. Figure 4(a) and (b) shows the migration results by using the uniform sampling method and the 3D Lloyd's algorithm respectively. In Figure 4(a), the steeply dipping salt flank A and the salt boundary B, as well as the steeply dipping fault C are mispositioned due to the inaccuracy of the reference parameters selected by the uniform sampling. In Figure 4, with the reference parameters selected by the 3D Lloyd's algorithm, all the three parts are correctly positioned and well imaged.

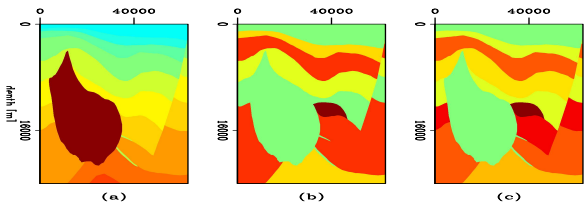

Figure 3: Synthetic anisotropy model. (a) Vertical velocity v; (b) anisotropy parameter δ; (c) anisotropy parameter ε.

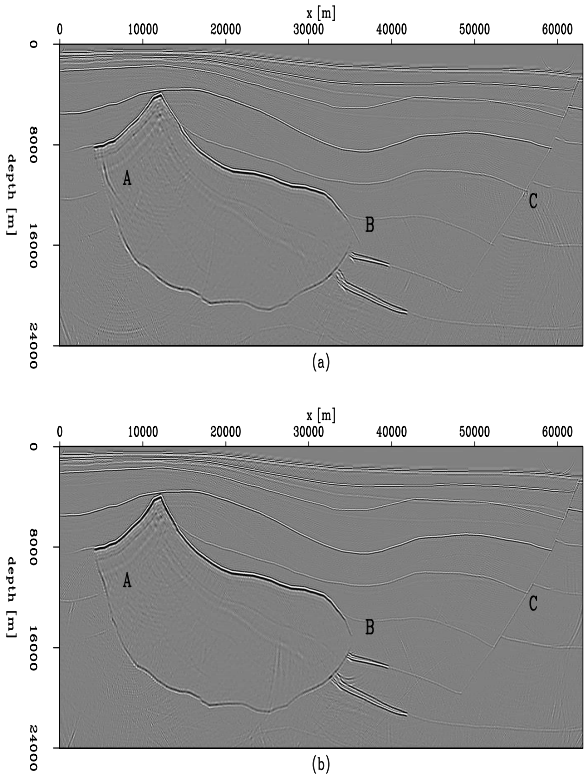

Figure 4: 2D anisotropic zero-offset migration results. (a) Reference parameters selected by the uniform sampling; (b) reference parameters selected by the 3D Lloyd's algorithm.

For the real data set MC311, which is a 2D slice of a 3D survey, we use the same strategy discussed above for selecting the reference parameters for both methods. Then the data set is downward continuated separately for each reference-parameter vector by the source-receiver anisotropic DSR extrapolator with split-step corrections on velocities, and a linear interpolation is performed on those reference wavefields to generate a single wavefield, followed by the implementation of the imaging condition $t = 0$ and $h = 0$ to obtain the final image, where t is the two-way travel time and h

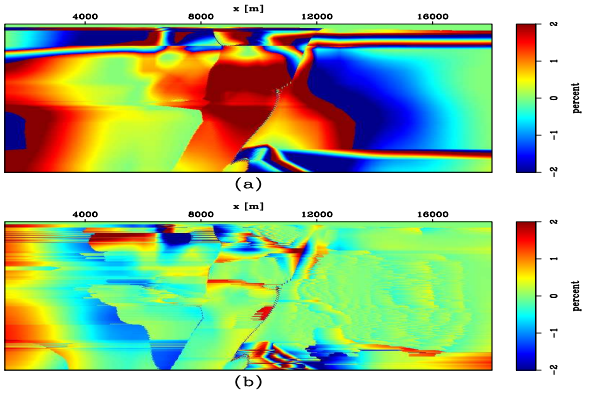

Figure 5: Error map between the actual velocities and the reference velocities (the vertical axes are depths). Both maps are shown in the same scale (percentage). (a) By uniform sampling method; (b) by Lloyd's algorithm.

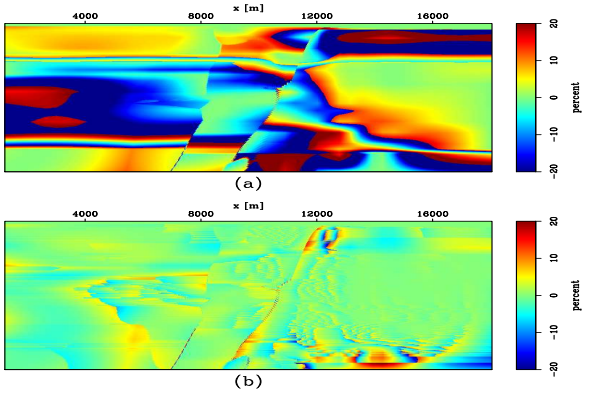

Figure 6: Error map between the actual δ and the reference δ (the vertical axes are depths). Both maps are shown in the same scale (percentage). (a) By uniform sampling method; (b) by Lloyd's algorithm.

is the half-offset. In the DSR migration process, most of the computation time is spent on the downward continuation step. In this particular case with the total number of depth levels $nz = 410$, we must perform $410 \times 27 = 11{,}070$ downward continuations for the uniform sampling method. After selecting by the modified Lloyd's algorithm, however, the total number of downward continuations reduces to 4,952, reducing the computation time by about 54%. Figures 5–7 show the error maps between the actual model and the selected reference parameters both by the uniform sampling method and the modified 3D Lloyd's method. Obviously, using Lloyd's method, we obtain much smaller differences between the actual model and the reference parameters.

Figure 8(a) shows the 2D prestack migration result of the conventional approach, while Figure 8(b) shows the result of using the modified 3D Lloyd's algorithm for reference-parameter selections. Though in both cases, all reflectors are nicely imaged, we can still identify the differences between Figure 8(a) and 8(b). Using the 3D Lloyd's algorithm yields a clearer top boundary of the salt body (portion A) as well as a more focused and continuous steeply dipping salt flank (portion B). One thing needed for an extra emphasis is that the computational cost by using Lloyd's algorithm is only half of that by using the conventional method.

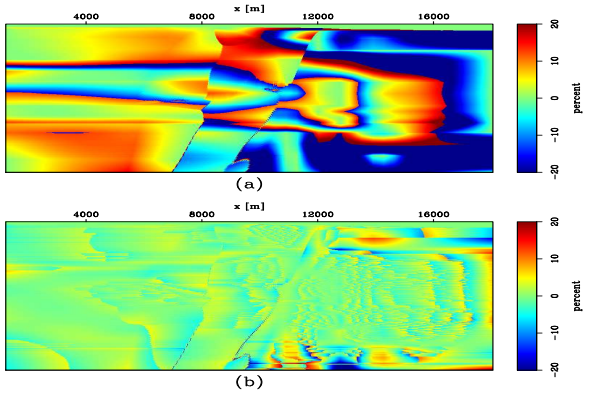

Figure 7: Error map between the actual η and the reference η (the vertical axes are depths). Both maps are shown in the same scale (percentage). (a) By uniform sampling method; (b) by Lloyd's algorithm.

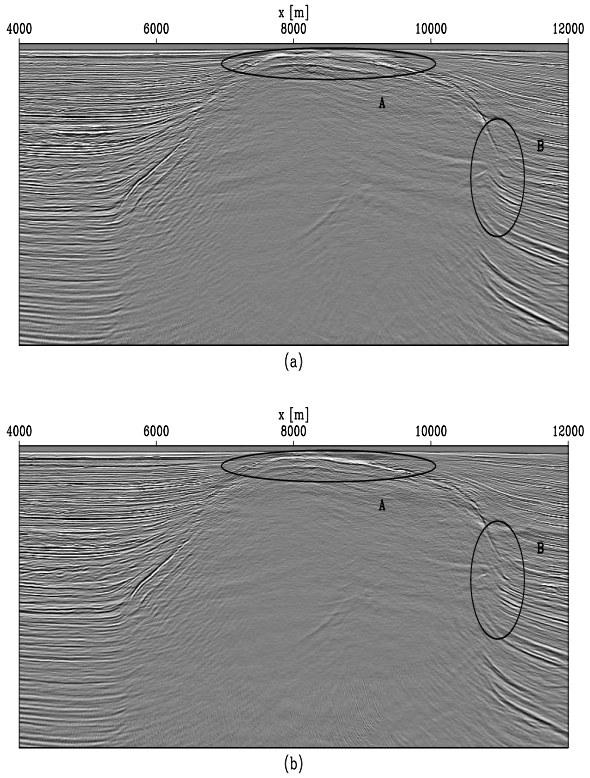

Figure 8: Anisotropic prestack migration result (the vertical axes are depths). (a) Reference parameters selected by the uniform sampling method; (b) reference parameters selected by the modified 3D Lloyd's algorithm. The computational cost for (b) is only half of that for (a).

CONCLUSION

By extending the 1D Lloyd's algorithm to 3D, we have presented a method for selecting reference-anisotropy parameters for wavefield downward continuation. The modified Lloyd's algorithm is a dynamic process that automatically determines the fewest reference parameters necessary to best characterize the actual model for each depth level. It eliminates reference parameters that are redundant or contribute little to the result. Therefore, by using the modified Lloyd's algorithm, it is possible for us to obtain an optimum migration result with relatively few reference parameters, significantly reducing the computational cost compared with the uniform sampling method. Our test on synthetic and real data sets shows that reference-anisotropy parameters selected by the modified 3D Lloyd's algorithm characterize the actual model well, and that migrating with those reference parameters leads to an image with higher quality, at lower cost, than the conventional uniform sampling method.

ACKNOWLEDGMENTS

We would like to thank Amerada Hess for making the synthetic data set available and ExxonMobil for making the real data set available.

REFERENCES

Baumstein, A. and J. E. Anderson, 2003, Wavefield extrapolation in laterally varying vti media: 73rd Ann. Internat. Mtg., Soc. of Expl. Geophys., Expanded Abstracts, 945–948.

Biondi, B., 2002, Stable wide-angle Fourier finite-difference downward extrapolation of 3-D wavefields: Geophysics, **67**, no. 03, 872–882.

Clapp, R. G., 2004, Reference velocity selection by a generalized lloyd method: 74th Ann. Internat. Mtg., Soc. of Expl. Geophys., Expanded Abstracts, 981–984.

Clapp, R. G., 2006, A modified lloyd algorithm for characterizing vector fields: SEP–**124**.

Gazdag, J. and P. Sguazzero, 1984, Migration of seismic data by phase-shift plus interpolation: Geophysics, **49**, no. 02, 124–131.

Kessinger, W., 1992, Extended split-step Fourier migration: Soc. of Expl. Geophys., 62nd Ann. Internat. Mtg, 917–920.

Lloyd, S. P., 1982, Least squares quantization in pcm: IEEE Transactions on Information Theory.

Popovici, A. M., 1996, Prestack migration by split-step DSR: Geophysics, **61**, no. 05, 1412–1416.

Rousseau, J. H. L., 1997, Depth migration in heterogeneous, transversely isotropic media with the phase-shift-plus-interpolation method: Soc. of Expl. Geophys., 67th Ann. Internat. Mtg, 1703–1706.

Stoffa, P. L., J. T. Fokkema, R. M. de Luna Freire, and W. P. Kessinger, 1990, Split-step Fourier migration: Geophysics, **55**, no. 04, 410–421.

Thomsen, L., 1986, Weak elastic anisotropy: Geophysics, **51**, no. 10, 1954–1966.

Tsvankin, I., 2001, Seismic signatures and analysis of reflection data in anisotropic media: Pergamon.